Rare Met. (2022) 41(2):580–593
https://doi.org/10.1007/s12598-021-01826-w

RARE METALS

ORIGINAL ARTICLE

Antibacterial property of a gradient Cu-bearing titanium alloy by laser additive manufacturing

Dong-Yang Fan, Zhe Yi, Xu Feng, Wen-Zhi Tian, Da-Ke Xu, A. M. Cristino Valentino, Qiang Wang*, Hong-Chen Sun*

Received: 22 April 2021 / Revised: 14 May 2021 / Accepted: 3 June 2021 / Published online: 27 September 2021

Abstract *Streptococcus mutans* (*S. mutans*) is the most common cariogenic bacteria and causes caries by forming biofilms. A novel gradient Cu-bearing titanium alloy (TC4-5Cu/TC4) was manufactured using selective laser melting (SLM) technology for dental applications, which is anticipated to inhibit the formation of biofilm. In this study, the released concentration of copper ions in both minimum inhibitory concentration (MIC) and minimum bactericidal concentration (MBC) was tested in order to assess the antibacterial property of the alloy against planktonic *S. mutans*, and the antibacterial and antibiofilm efficiencies of TC4-5Cu/TC4 alloy against sessile *S. mutans* were evaluated via quantitative antibacterial tests and biofilm determination. Reverse transcription polymerase chain reaction (RT-PCR) was performed to analyze the expression of biofilm-related genes (*gtfB*, *gtfC*, *gtfD*, *ftf* and *gbpB*) and acid production-related gene (*ldh*). The results suggested that the MIC and MBC of Cu^{2+} were much higher than the release concentration of copper ions of the alloy, which was consistent with the lack of antibacterial effect against planktonic bacteria. On the contrary, TC4-5Cu/TC4 alloy exhibited significant bactericidal property against the sessile bacteria and efficient biofilm-restrained ability, and all genes detected in this research were down-regulated. The results indicated that the TC4-5Cu/TC4 alloy suppressed biofilm formation and the sessile bacterial viability by down-regulating biofilm-related genes.

Keywords Copper; Titanium alloys; Biofilm; Antibacterial property; *Streptococcus mutans*

1 Introduction

Dental caries is a common oral disease, which is listed as one of the three key human diseases for prevention and treatment by the World Health Organization. *Streptococcus mutans (S. mutans)* is the most important cariogenic bacteria, which causes caries by forming dental plaque biofilm on the tooth surface [1]. The formation process of dental plaque biofilm includes saliva acquired membrane formation, bacterial adhesion and coaggregation, and biofilm maturation [2]. The biofilm is a stable and nutrient-rich system, and the bacteria in the biofilm are wrapped and protected by extracellular polysaccharides (EPS) [3]. Therefore, the resistance and pathogenicity of sessile bacteria are enhanced, compared with planktonic bacteria [4, 5]. The EPS of *S. mutans* mainly consist of glucan and fructan, which are synthesized compounds catalyzed by glucosyltransferase (GTF) and fructosyltransferase (FTF) [6]. Based upon the role of the synthesized dextran, GTF encoded by the *gtf* gene is divided into 3 types, including GTFB, GTFC, and GTFD. GTFB catalyzes the synthesis of water-insoluble glucan by sucrose, which facilitates mutual

D.-Y. Fan, Z. Yi, X. Feng, W.-Z. Tian, Q. Wang*, H.-C. Sun*
School and Hospital of Stomatology, China Medical University, Liaoning Provincial Key Laboratory of Oral Diseases, Shenyang 110002, China
e-mail: mfqwang@cmu.edu.cn

H.-C. Sun
e-mail: sunhongchen@cmu.edu.cn

D.-K. Xu
Shenyang National Laboratory for Materials Science, Key Laboratory for Anisotropy and Texture of Materials (Ministry of Education), School of Materials Science and Engineering, Northeastern University, Shenyang 110819, China

A. M. Cristino Valentino
Department of Electromechanical Engineering, University of Macau, Avenida da Universidade, Taipa, Macao, China

adhere between *S. mutans* cells and contributes to stabilizing the biofilm [7]. GTFC is capable of catalyzing the formation of water-insoluble and alkali-soluble glucans, which are responsible for the adhesion of *S. mutans* to the saliva acquired membrane and improve the acid resistance of bacteria [8, 9]. The water-soluble glucan is synthesized by GTFD and is also required for the adhesion of *S. mutans* to the saliva acquired membrane [10, 11]. FTF, the product of the *ftf* gene, plays a significant role in catalyzing fructose into fructan, which can provide energy reserves and maintain biofilm stability during periods of nutrient deficiency [12, 13]. Furthermore, glucan-binding proteins (GbpB) encoded by the *gbpB* gene are also closely related to the formation and stability of biofilm. They can enhance the affinity of *S. mutans* and glucan, maintain the structure of the bacterial cell wall, and promote the connection of *S. mutans* cells into chains [14, 15]. In addition to the formation of biofilms, aciduricity is also an integral factor in the pathogenicity of *S. mutans*. Lactic acid synthesized by lactate dehydrogenase (LDH) is the main acidic metabolite of *S. mutans*, which directly leads to tooth demineralization [13, 16].

Bacterial adhesion is the critical stage of biofilm formation and tooth demineralization, especially the dental tissues around the oral treatment appliance are more likely to attach to bacteria [17]. At present, the main clinical strategies for removing biofilm are mechanical methods and mouthwashes. However, mechanical methods are difficult to clean sufficiently due to the obstacles of appliances. In addition, mouthwashes may cause mucosa discoloration, impaired taste perception, and mucosal burning sensation [18, 19]. Therefore, it is essential to develop antibacterial materials in order to solve the problem in a fundamental level.

Titanium alloys have been widely used in the field of stomatology due to their excellent biocompatibility and mechanical properties. However, it cannot inhibit the adhesion of bacteria and the formation of biofilms. Copper and silver are widely applied in antibacterial fields due to well-known for their antibacterial property [20–22]. However, heavy metals like silver are toxic, while copper is an essential trace element in human body. Therefore, copper is more suitable for medical materials [23]. Moreover, copper has been registered as a metal antibacterial material by the U.S. Environmental Protection Agency [24, 25]. Previous studies have shown that the addition of copper into titanium alloys provided good antibacterial properties against *Staphylococcus aureus* (*S. aureus*) and *Escherichia coli* (*E. coli*) [26, 27].

At present, the common methods of adding copper content to titanium alloys include surface modification to prepare Cu-bearing coatings and overall modification to manufacture cast Cu-bearing titanium alloys [28–30]. Typical surface modification techniques generally have the shortcomings of coating falling off easily and cumbersome production process [31–33]. Meanwhile, the cast Cu-bearing titanium alloy cannot guarantee completely unchanged mechanical properties, and the casting processing also increases the manufacturing time cost and labor error [34]. Thus, in order to overcome the above shortcomings, a novel Cu-bearing titanium alloy was designed and fabricated using selective laser melting (SLM) with computer-aided design data (CAD) modeling.

S. mutans is one of the most common pathogens in the oral cavity, for its strongest ability of acid production and biofilm formation in oral streptococcus [35, 36]. For exploring whether the new Cu-bearing titanium alloy is suitable for dental appliance, it is necessary to investigate the antibacterial activity of the alloy against *S. mutans*. In this research, the alloy was based on commercial Ti6Al4V powder and prepared with SLM, and for the last 80 μm, the powder was replaced by commercial Ti6Al4V5Cu powder, resulting in a gradient copper-bearing titanium alloy TC4-5Cu/TC4. The SLM processed TC4-5Cu/TC4 alloy was evaluated for its antibiofilm ability against *S. mutans*, through quantitative antibacterial test, biofilm detection and PCR assay. In addition, the contact angle, roughness, and Cu^{2+} release concentration of the alloy were tested to evaluate its physical and chemical properties.

2 Experimental

2.1 Sample preparation

The preparation parameters of SLMed TC4-5Cu/TC4 alloy are displayed in Table 1, which were consistent with previous study [37]. At first, commercial Ti6Al4V powder (Fig. 1a) was fabricated into TC4 alloy (Fig. 1c) with dimension of 10 mm × 10 mm × 2 mm using SLM. Then, it was replaced with Ti6Al4V5Cu powder (Fig. 1b) to further produce a 80-μm-thick TC4-5Cu alloy, resulting in a gradient TC4-5Cu/TC4 alloy (Fig. 1d). Figure 1c, d exhibits the elemental composition of Ti6Al4V powder and Ti6Al4V5Cu powder, tested by energy dispersive spectroscopy (EDS, Zeiss Merlin Compact, Zeiss, Germany). Before the test, each sample was ultrasonically cleaned in acetone, distilled water, and ethanol for about 15 min, followed by drying at room temperature to prepare for the experiment. The surface topography and components of TC4-5Cu/TC4 alloys mounted in epoxy resin were measured by scanning electron microscope (SEM, Zeiss Merlin Compact, Zeiss, Germany) and EDS (Zeiss Merlin Compact, Zeiss, Germany).

Table 1 Preparation parameters of TC4-5Cu/TC4 alloy

Scanning speed/ ($mm \cdot s^{-1}$)	Laser power/ W	Spot diameter/ μm	Scanning interval/ μm	Layer thickness/ μm
1500	260	70	45	30

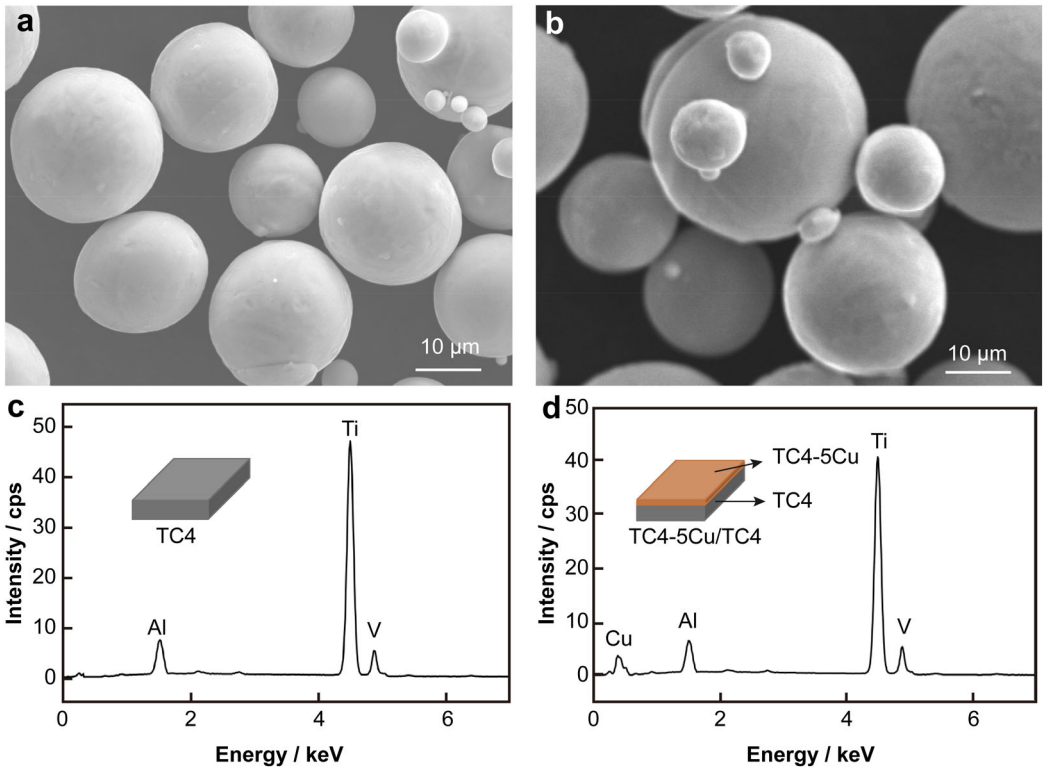

Fig. 1 SEM images of **a** Ti6Al4V powder and **b** Ti6Al4V5Cu powder; EDS mappings of **c** Ti6Al4V powder and **d** Ti6Al4V5Cu powder (insets being schematic diagrams of TC4 and TC4-5Cu/TC4 alloys)

2.2 Surface characterization

The contact angles of samples were measured with a pendant drop method using a contact angle instrument (TBU 95, DataPhysics, Germany). At room temperature, 0.2 μl deionized water was dropped onto the surface of specimens. After the drop stabilizes, the contact angle was detected and the image was recorded. The roughness of the alloys was tested by a roughness meter (SJ-210, Surftest, Japan). The measurements of samples were conducted in triplicate, respectively.

2.3 Cu^{2+} release

According to ISO standard 10993-12, the TC4-5Cu/TC4 samples were immersed in normal saline at 37 °C (1.25 $cm^2 \cdot ml^{-1}$). The concentration of copper ions was measured by an inductively coupled plasma mass spectrometry (7800 ICP-MS, Agilent, USA) at 1, 3, 7, 14 and 28 days. At least three samples were tested at each time point.

2.4 Bacterial strain and medium

The bacteria used for antibacterial experiments were *S. mutans* (ATCC 25175). First of all, the strain was transferred from the frozen glycerol to a sterile brain–heart infusion (BHI, pH = 7.0) ager (Meilun, China) plate. After cultured anaerobically (90% N_2 and 10% CO_2) for 72 h at 37 °C, the *S. mutans* colonies were transferred to 50 ml sterile BHI liquid medium and incubated under the same conditions for 20 h [38].

2.5 MIC and MBC concentrations determination

The improved broth dilution method approved by Clinical and Laboratory Standards Institute (CLSI) was performed to determine the MIC and MBC of Cu^{2+}. The equal volume

(500 μl) of *S. mutans* suspension and $CuCl_2$ BHI medium solution were mixed together in a 24-well plate (n = 3, i.e. three parallel experimental groups were set up for each ion concentration). The diluted Cu^{2+} concentration was 0, 3.5, 7.0, 14.0, 28.0, 56.0, 112.0, 224.0, 448.0 mg·L^{-1}, and the bacterial concentration was 3×10^5 CFU·ml^{-1}. The well plate was incubated anaerobically for 24 h at 37 °C and observed to confirm the MIC value. MIC was recognized as the lowest Cu^{2+} concentration without visible bacteria occurred. After that, the bacterial suspension was transferred to a 1.5 ml Eppendorf (EP) tube and vortexed. Each 100 μl the mixed solution was inoculated on the BHI ager plate, with further incubation for 72 h. MBC was described as the lowest concentration of Cu^{2+} without macroscopic colonies on the culture plate.

2.6 Antibacterial efficacy of TC4-5Cu/TC4

The antibacterial efficacy of TC4-5Cu/TC4 against *S. mutans* was investigated by the visual plate counting method, and the schematic representation of the experimental process is shown in Fig. 2. TC4-5Cu/TC4 and TC4 alloys (10 mm × 10 mm × 2 mm) were immersed in 1 ml bacterial suspension (3×10^5 CFU·ml^{-1}) in a 24-well plate and cultured at 37 °C for 1 and 3 days, respectively. The bacterial suspension without sample served as blank control.

2.6.1 Antibacterial effect on planktonic S. mutans

At predetermined time intervals, the bacterial suspension was collected into a 1.5 ml Eppendorf tube and vortexed for 1 min. The pH of each suspension was determined by a pH meter (FE28-FiveEasy Plus™, METTLER TOLEDO). Then, after continuous dilution in phosphate buffered saline (PBS, pH = 7.0), 100 μl suspension from each tube was inoculated on the BHI agar plate. After further incubation anaerobically at 37 °C for 48 h, the viable bacterial colonies were counted.

2.6.2 Antibacterial effect on sessile S. mutans

At the scheduled time, the samples were transferred to sterile PBS and lightly rinsed to remove the planktonic bacteria on the surface. Next, the coupons were put into 5 ml EP tubes containing 1 ml PBS. The suspension was vortexed for 1 min and gradually diluted with PBS. Subsequently, 100 μl bacterial suspension from each tube was spread on the plate and incubated at 37 °C for 48 h. The bacterial colonies on the plate were counted and analyzed. Finally, the antibacterial rate was calculated with Eq. (1):

$$R_1 = \left(N_{TC4} - N_{TC4-5Cu/TC4}\right)/N_{TC4} \times 100\% \quad (1)$$

where R_1 is antibacterial rate, and N is the number of bacteria colonies.

2.7 SEM observation of biofilm

The morphology of sessile bacteria in the biofilm was observed by SEM. At first, the sterile samples (10 mm × 10 mm × 2 mm) were soaked in the liquid medium containing *S. mutans* according to the above manner. After cultured for 1 and 3 days, the samples were washed gently

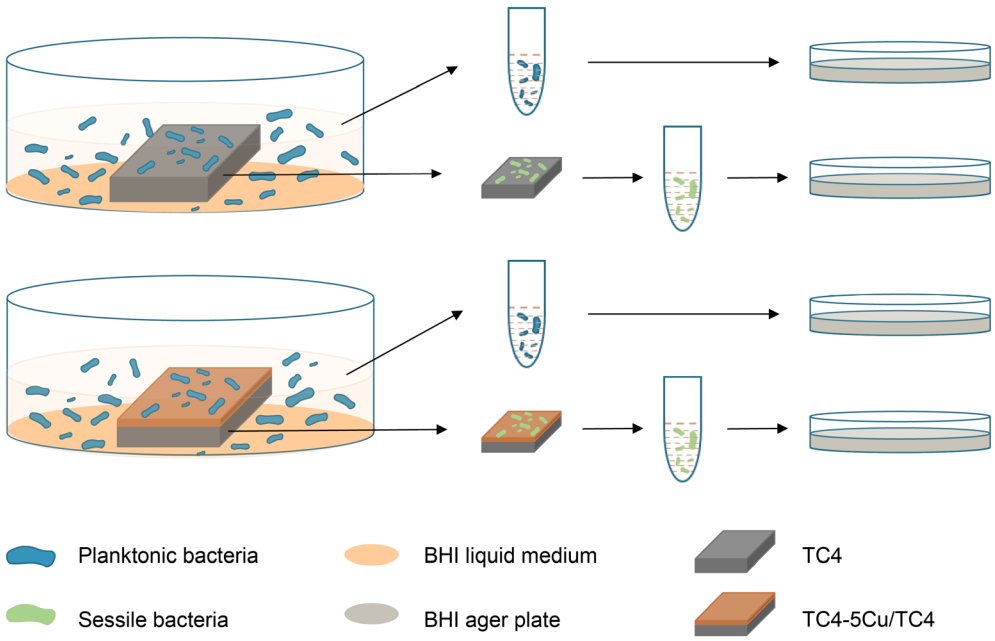

Fig. 2 Schematic diagram of visual plate counting method

with PBS to remove planktonic bacteria and then immersed in 2.5% glutaraldehyde at 4 °C for 4 h. Next, the specimens were dehydrated for 10 min in a series of ethanol solutions (50%, 60%, 70%, 80%, 90%, 95% and 100%; *v*/*v*) and dried at room temperature. Finally, the samples were observed by SEM after spraying with a gold layer [39].

2.8 Live/dead biofilm staining assay

The biofilm and bacterial viability of *S. mutans* on the coupons were studied by a confocal laser scanning microscopy (CLSM, Olympus FV3000, Japan). Bacteria and samples were prepared according to the previously mentioned methods. After 1 and 3 days, the coupons were rinsed lightly with PBS to remove unattached bacteria. Next, the bacterial biofilms were stained for 20 min in the dark, using the LIVE/DEAD BacLight bacterial viability kit (Invitrogen-Eugene, USA), which contains SYTO-9 dye and PI dye. SYTO-9 labeled live bacteria with intact membranes fluorescent green, while PI marked dead bacteria with damaged membranes in fluorescent red [40]. Then, the ImageJ software was used to analyze the proportion of dead cells in the images. After that, the stained bacteria were investigated by the CLSM, and the biofilms thickness was measured with the *Z*-axis scanning. Equation (2) was used to determine the antibiofilm rate:

$$R_2 = \left(t_{\mathrm{TC4}} - t_{\mathrm{TC4-5Cu/TC4}}\right)/t_{\mathrm{TC4}} \times 100\% \quad (2)$$

where R_2 is antibiofilm rate, and t is thickness.

2.9 Biofilm detection by crystal violet staining

The antibiofilm effects of samples were researched by crystal violet staining [41]. After incubated for 1 and 3 days, the samples were submerged in PBS to remove free-floating bacteria. Then, the coupons were immobilized in methanol for 15 min and dried at room temperature for 30 min. The sessile bacteria were stained with 0.1% crystal violet for 10 min. After that, the samples were washed with distilled water to remove excess crystal violet and dried at room temperature. Absolute ethyl alcohol was used to elute the dye bound to the biofilm, and then the absorbance was recorded at 600 nm with a microplate reader (Tecan, Salzburg, Austria). The antibiofilm rate was calculated with Eq. (3):

$$R_3 = \left(\mathrm{OD}_{\mathrm{TC4}} - \mathrm{OD}_{\mathrm{TC4-5Cu/TC4}}\right)/\mathrm{OD}_{\mathrm{TC4}} \times 100\% \quad (3)$$

2.9.1 RT-PCR analysis

The RT-PCR assay was used to analyze the effect of TC4-5Cu/TC4 on *S. mutans* genes expression. The samples were soaked in 1 ml culture media containing 3×10^8 CFU·ml^{-1} bacteria for 1 and 3 days. Followed by washing away the planktonic bacteria with PBS, and the sessile bacteria were collected in 1 ml RNAprotect bacteria reagent (Qiagen GmbH, Hilden, Germany). After centrifugation at 4 °C, the total RNA of sessile bacteria was extracted using RNAiso Plus (TaKaRa, Japan), and cDNA was synthesized using Hifair® II 1st Strand cDNA Synthesis Kit (Yeasen, Shanghai, China). The reverse transcription conditions were 5 min at 25 °C, 30 min at 42 °C, and 5 min at 85 °C. The RT-PCR was implemented with Hieff® qPCR SYBR green master mix (Yeasen, Shanghai, China) in a QuantStudio 3 real-time PCR system (Applied Biosystems, Thermo Fisher, Singapore). The amplification conditions were 95 °C for 5 min followed by 40 cycles at 95 °C for 10 s and 60 °C for 30 s. The genes expression levels of *gtfB*, *gtfC*, *gtfD*, *gbpB*, *ftf*, and *ldh* were tested, and the 16S rRNA gene was internal control.

2.9.2 Statistical analysis

The obtained data were analyzed by the t test and one-way analysis of variance (ANOVA) via GraphPad Prism (version 7.00) software (GraphPad Software, San Diego, California, USA) to assess statistical differences. All experiments were performed at least three times independently, and the results were described as the mean values ± standard deviation (SD), respectively. The statistical significance level was set as 95%.

3 Results

3.1 Characterization studies

Figure 3 and Table 2 demonstrate the surface morphology and elemental composition percentage, exhibiting that the alloy surface was mainly composed of Ti, Al, V and Cu, and all the constituent elements were evenly distributed. Cross-sectional morphology of TC4-5Cu/TC4 in Fig. 4 shows that there was no obvious boundary between the TC4-5Cu alloy on the surface and the TC4 alloy on the bottom. According to EDS mapping, the distribution of copper element on the alloy surface was within about 80 μm, confirming that the samples used were TC4-5Cu/TC4 alloys.

Figure 5 identifies that the hydrophilicity and roughness of TC4 and TC4-5Cu/TC4 were basically the same, and the contact angles of TC4 and TC4-5Cu/TC4 alloys were 78.07° ± 1.34° and 81.77° ± 1.22° (Fig. 5a), while the roughness values were (1.69 ± 0.06) μm and (1.66 ± 0.03) μm (Fig. 5b). The difference between the two groups of data was not statistically significant. In order to research the biological safety of TC4-5Cu/TC4 alloy, the

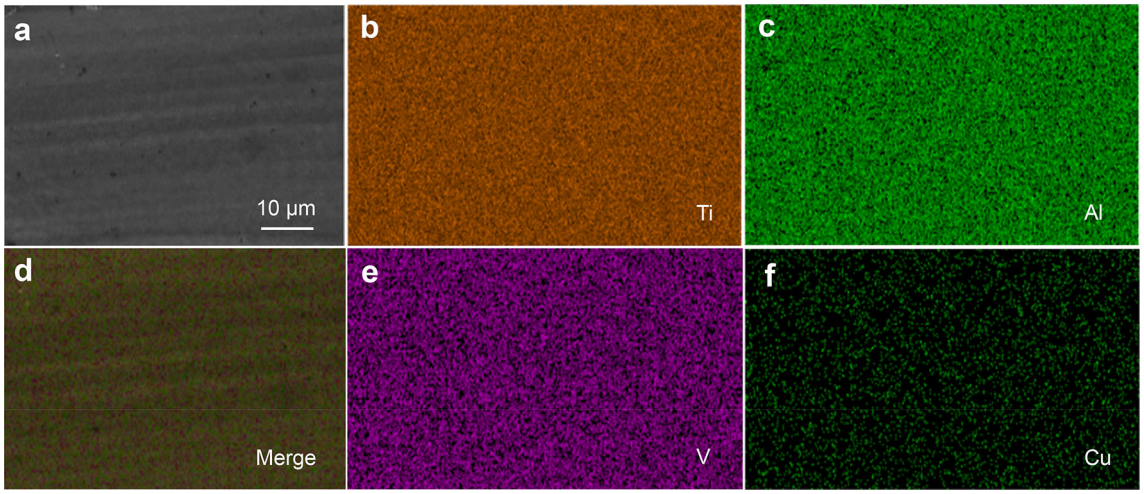

Fig. 3 **a** Surface morphology and **b–f** EDS elemental mappings of TC4-5Cu/TC4 alloy

Table 2 Elemental composition percentage of TC4-5Cu/TC4 alloy

Element	Ti	Al	V	Cu
w/wt%	84.82	5.14	4.04	6.01
x/at%	82.94	8.92	3.72	4.43

Cu^{2+} release concentration and rate of TC4-5Cu/TC4 alloy in normal saline were analyzed. As shown in Fig. 5c, Cu ions were constantly released within 28 days, and the highest concentration was (18.73 ± 0.87) $\mu g \cdot L^{-1}$. The maximum release rate of copper ions was about 2.53 $\mu g \cdot L^{-1} \cdot day^{-1}$ on the first day, and then the rate gradually decreased to 0.44 $\mu g \cdot L^{-1} \cdot day^{-1}$ on the 28th day.

3.2 MIC and MBC values

The purpose of this experiment was to investigate whether the Cu^{2+} released concentration by TC4-5Cu/TC4 alloy reached MIC and MBC of Cu^{2+}. Figure 6a presents that the 28.0 $mg \cdot L^{-1}$ was the minimum Cu^{2+} concentration free of macroscopic bacteria in the solution, and Fig. 6b exhibits that 56.0 $mg \cdot L^{-1}$ was the lowest Cu^{2+} concentration without visible colonies occurred on the BHI ager plate. It indicated that the MIC and MBC of Cu^{2+} against *S. mutans* were 28.0 and 56.0 $mg \cdot L^{-1}$ (Fig. 6a).

3.3 Antibacterial activities against planktonic bacteria and sessile bacteria

Figure 7 exhibits the planktonic and sessile *S. mutans* colonies and pH value of liquid medium incubated for 1 and 3 days. In Fig. 7a, the abundant of bacterial colonies were observed on the BHI ager medium of all groups. Figure 7b presents that the number of planktonic bacteria in three groups was similar. In addition, the pH values of solutions were basically the same whether there was a sample or not (Fig. 7c). The antibacterial test of planktonic bacteria confirmed that TC4-5Cu/TC4 alloy had little antibacterial effect on unattached bacteria. Based on plate images in Fig. 7d, the number of colonies on TC4-5Cu/TC4 alloy was significantly less than that on TC4 alloy. Figure 7e demonstrates that the average antibacterial rate of the TC4-5Cu/TC4 alloy against sessile *S. mutans* for 1 and 3 days was ∼ 46.17% and 74.39%, respectively. The above results show that the fabricated TC4-5Cu/TC4 alloys had satisfactory antibacterial effect against sessile bacteria in biofilm, but limited antibacterial activity against planktonic bacteria.

3.4 SEM observation of sessile bacteria

In order to investigate the morphology of sessile bacteria in biofilm, SEM observation was carried out. Figure 8 reveals that when compared with TC4 alloy, the number and chain length of sessile *S. mutans* on TC4-5Cu/TC4 alloy were significantly inhibited. Multitudinous bacteria were observed on TC4 alloy. Furthermore, compared with the first day, the number of bacteria on the third day was similar, but the bacterial chain was much longer. The results support the idea that TC4 alloy had little antibacterial property. On the contrary, the number of bacteria on TC4-5Cu/TC4 alloy was less than that on TC4 alloy. Furthermore, most of the bacteria existed as short chains or single cells, and the bacterial chains on the third day were obviously shorter than those on the first day. Based on SEM observation, it was suggested that TC4-5Cu/TC4 alloy restrained biofilm formation and hindered the adhesion between *S. mutans*.

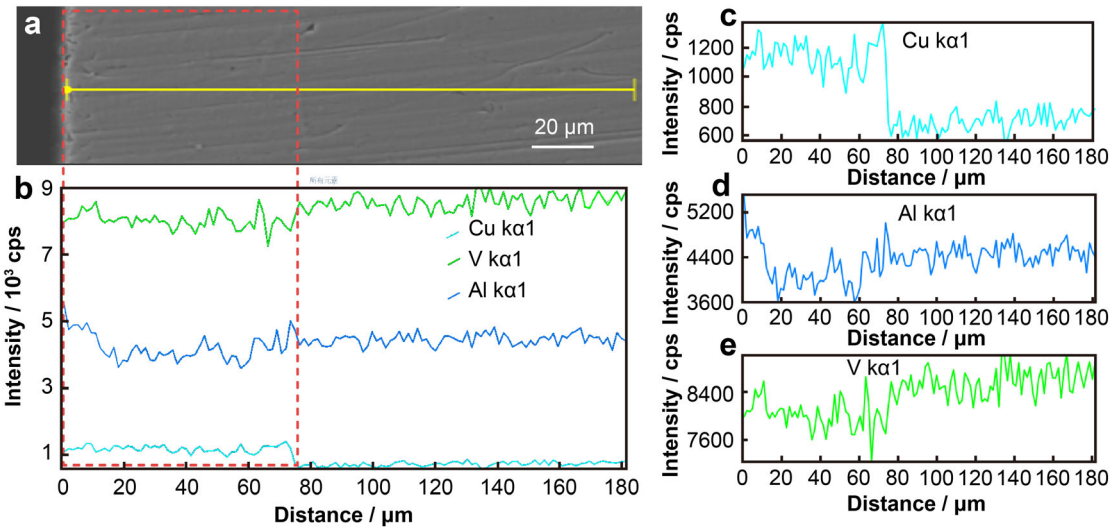

Fig. 4 **a** Cross-sectional SEM image and **b–e** EDS spectra of TC4-5Cu/TC4 alloy

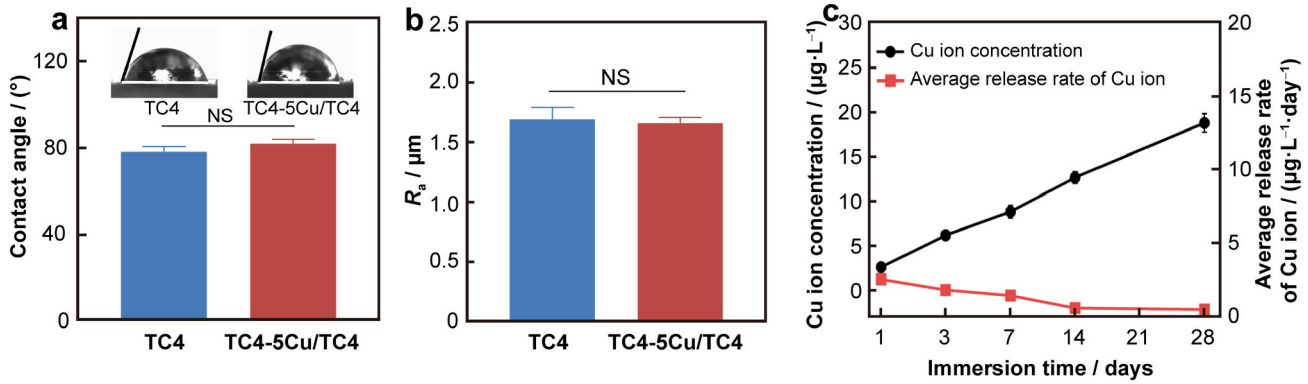

Fig. 5 **a** Water contact angles and typical images of water droplets on TC4 and TC4-5Cu/TC4 alloys; **b** roughness of TC4 and TC4-5Cu/TC4 alloys; **c** cumulatively leakage concentration and average release rates of Cu ions from TC4-5Cu/TC4 alloys in normal saline at 37 °C (NS: not statistically significant)

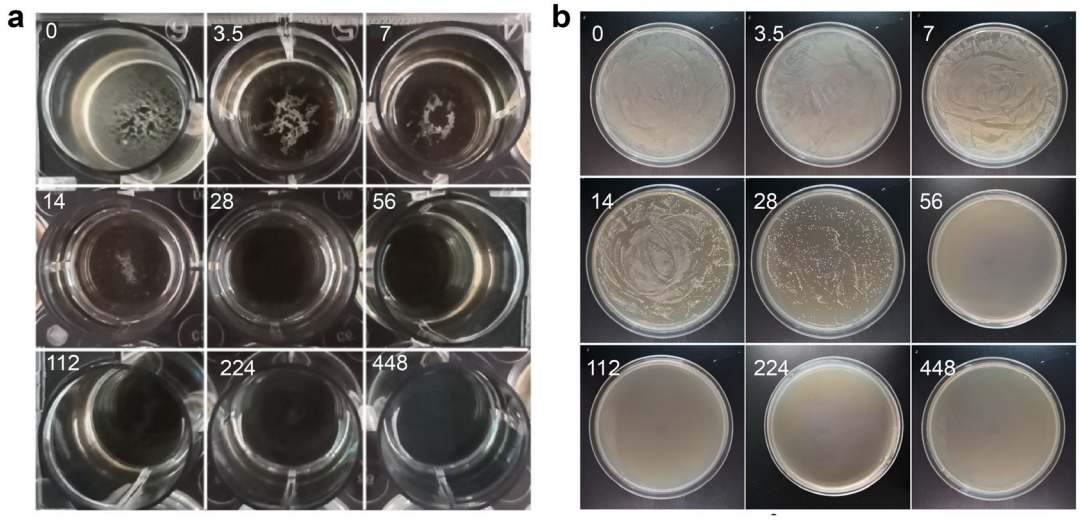

Fig. 6 **a** Macroscopic images of bacteria in liquid culture medium with different Cu^{2+} concentrations; **b** visible colonies on BHI ager plates (numbers ($mg \cdot L^{-1}$) in images representing concentration of copper ions)

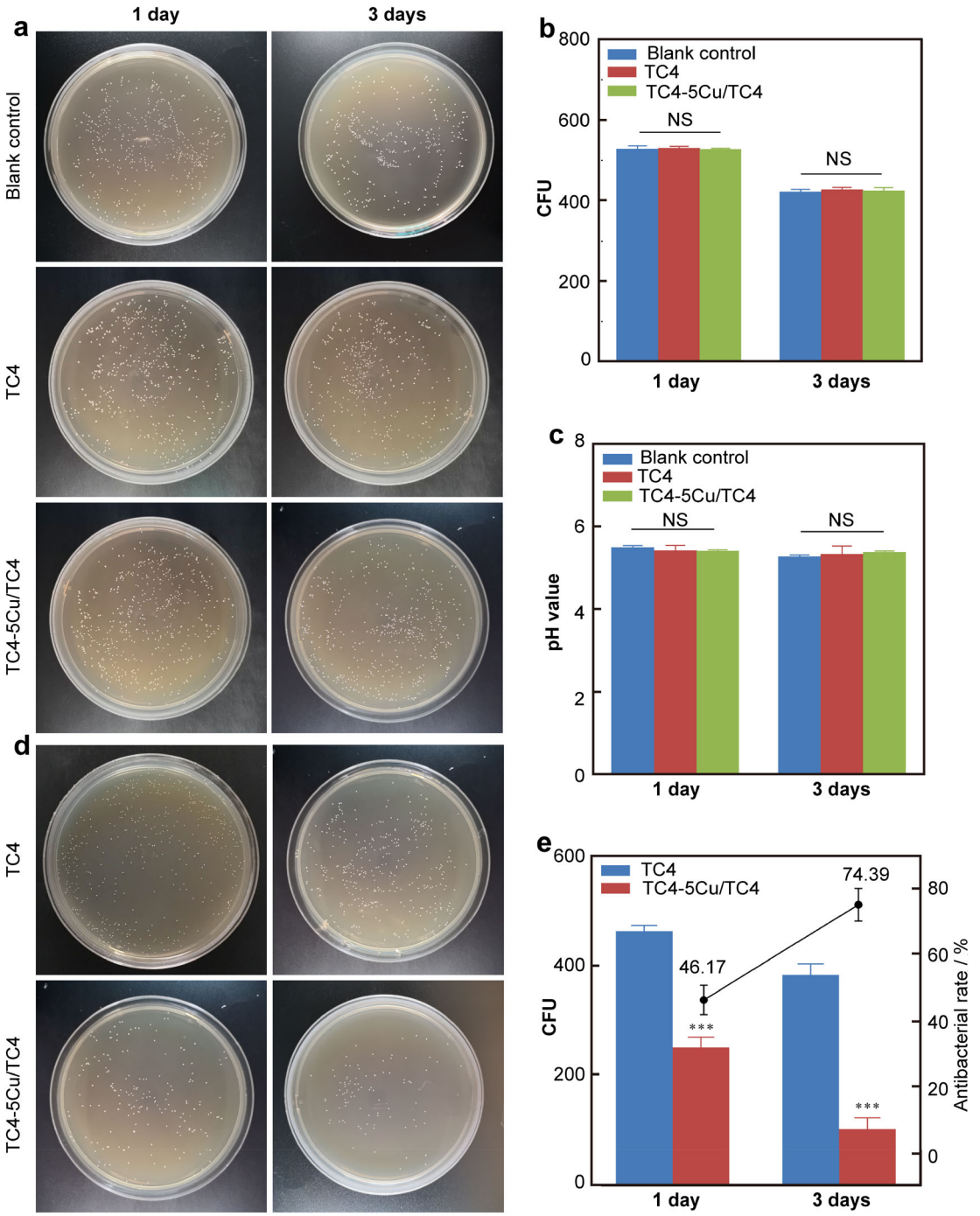

Fig. 7 Antibacterial activities of TC4-5Cu/TC4 alloy against planktonic and sessile bacteria: **a** planktonic *S. mutans* colonies after incubation for 1 and 3 days; **b** statistics of number of planktonic *S. mutans* colonies; **c** pH values of different liquid mediums after incubation for 1 and 3 days; **d** sessile *S. mutans* colonies on TC4 and TC4-5Cu/TC4 samples; **e** number of sessile *S. mutans* colonies from two groups of samples, and antibacterial rate of TC4-5Cu/TC4 alloy (***$p < 0.001$, NS: not statistically significant)

3.5 Sessile bacteria viability

Figure 9 shows live and dead staining of sessile bacteria on the samples. Figure 9a presents that numerous live bacteria stained as green adhered to the TC4 alloy. In contrast, the bacteria attached on the TC4-5Cu/TC4 alloy were mainly red-stained dead bacteria. The number of dead bacteria in the CLSM images was quantitatively analyzed by ImageJ software. The data in Fig. 9b indicated that the proportions of dead bacteria on TC4 alloy at 1 and 3 days were 3.97% ± 1.49% and 9.43% ± 1.76%, while those on TC4-5Cu/TC4 alloy were 67.67% ± 3.79% and

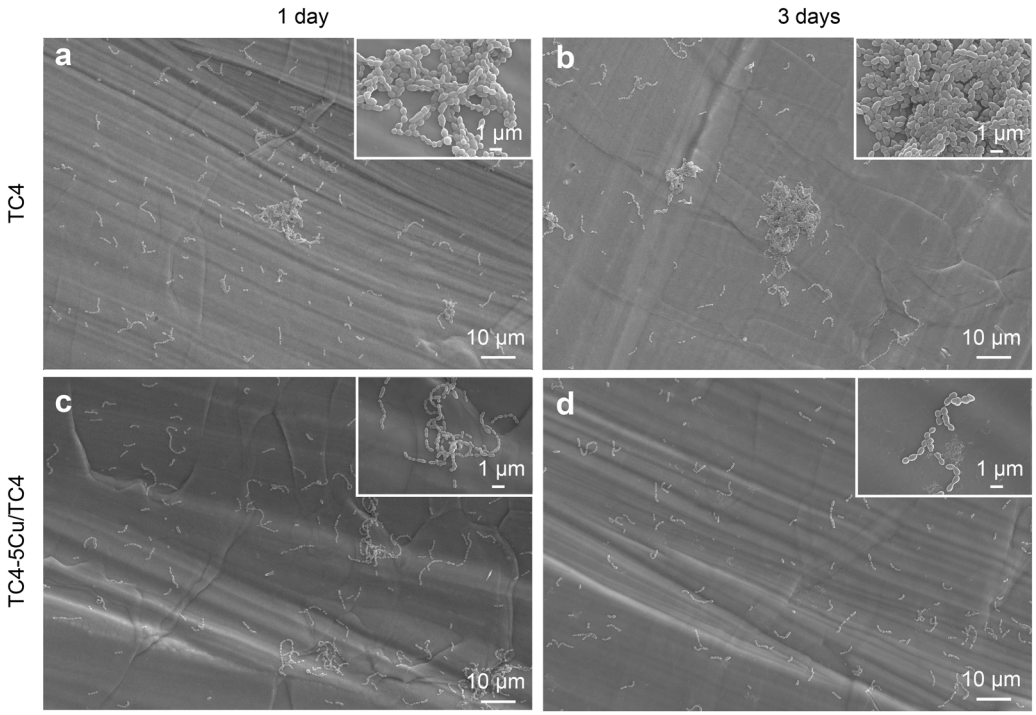

Fig. 8 SEM images and number of sessile *S. mutans* observation on **a, b** TC4 and **c, d** TC4-5Cu/TC4 alloys after culturing for 1 and 3 days

87.3% ± 5.62%, respectively. This result is consistent with the antibacterial trend of CLSM images.

The structure of biofilm was measured by *Z*-axis scanning of CLSM. Figure 9a clearly distinguishes the difference of biofilm thickness and the proportion of dead bacteria between the two samples. The average biofilm thicknesses of TC4 alloy on 1 and 3 days were (39.27 ± 1.71) μm and (32.83 ± 1.93) μm, respectively. However, the values of TC4-5Cu/TC4 alloy were (19.97 ± 0.92) μm and (13.16 ± 1.06) μm, respectively, which were much lower than the biofilm thickness on TC4 alloy (Fig. 9c). In addition, the average antibiofilm rates on the first day and third day were 41.48% ± 8.97% and 59.93% ± 2.03%, respectively. These results illustrate that TC4-5Cu/TC4 alloy could greatly suppress the activity of *S. mutans* and reduce the formation of bacterial biofilm.

3.6 Quantitative detection of biofilm

Crystal violet staining was performed to quantify bacteria biofilm formation. Figure 10a shows the absolute ethanol that dissolved the crystal violet bound to the biofilm. It was found that the solution color from TC4-5Cu/TC4 was more transparent. Consistently, the absorbance of stained *S. mutans* biofilm on the TC4-5Cu/TC4 alloy was much lower than that of TC4 alloy (Fig. 10b). Furthermore, the average antibiofilm rate on the first day and third day was 38.09% ± 4.41% and 63.58% ± 1.54%, respectively. Namely, the biofilm decrease degree on the third day was greater than that on the first day. This is similar to the trend in biofilm observed by CLSM, clarifying that TC4-5Cu/TC4 alloys restrain the formation of biofilms.

3.7 Effect on gene expression of sessile *S. mutans*

To study the effect of TC4-5Cu/TC4 alloy on the gene expression of *S. mutans*, PCR assay was carried out. The tested genes were mainly related to EPS synthesis and sucrose-dependent adhesion (*gtfB*, *gtfC*, *gtfD*, *ftf,* and *gbpB*). In addition, the gene *ldh* related to bacterial acidogenicity was also analyzed. Figure 10 clarifies that compared with TC4 alloy, TC4-5Cu/TC4 alloy significantly down-regulated the expression level of tested genes in sessile bacteria. Figure 10c presents that on the first day, the expression values of *gtfB*, *gtfC*, *gtfD*, *ftf*, *gbpB* and *ldh* genes of TC4-5Cu/TC4 alloy were about 40.02%, 37.44%, 66.37%, 90.99%, 38.26% and 48.87% that with TC4 alloy, respectively, while the values of the third day were ~ 31.52%, 22.03%, 45.79%, 30.93%, 28.31% and 44.05%, respectively (Fig. 10d). The relative fold expression of all genes on the third day of TC4-5Cu/TC4 alloy, especially *ftf* gene, was significantly lower than that on the first day. It is deduced that TC4-5Cu/TC4 alloy inhibits the expression of adhesion and aciduricity genes in *S. mutans* pathogenic genes, prevents bacterial biofilm formation at the genetic level, and reduces cariogenicity.

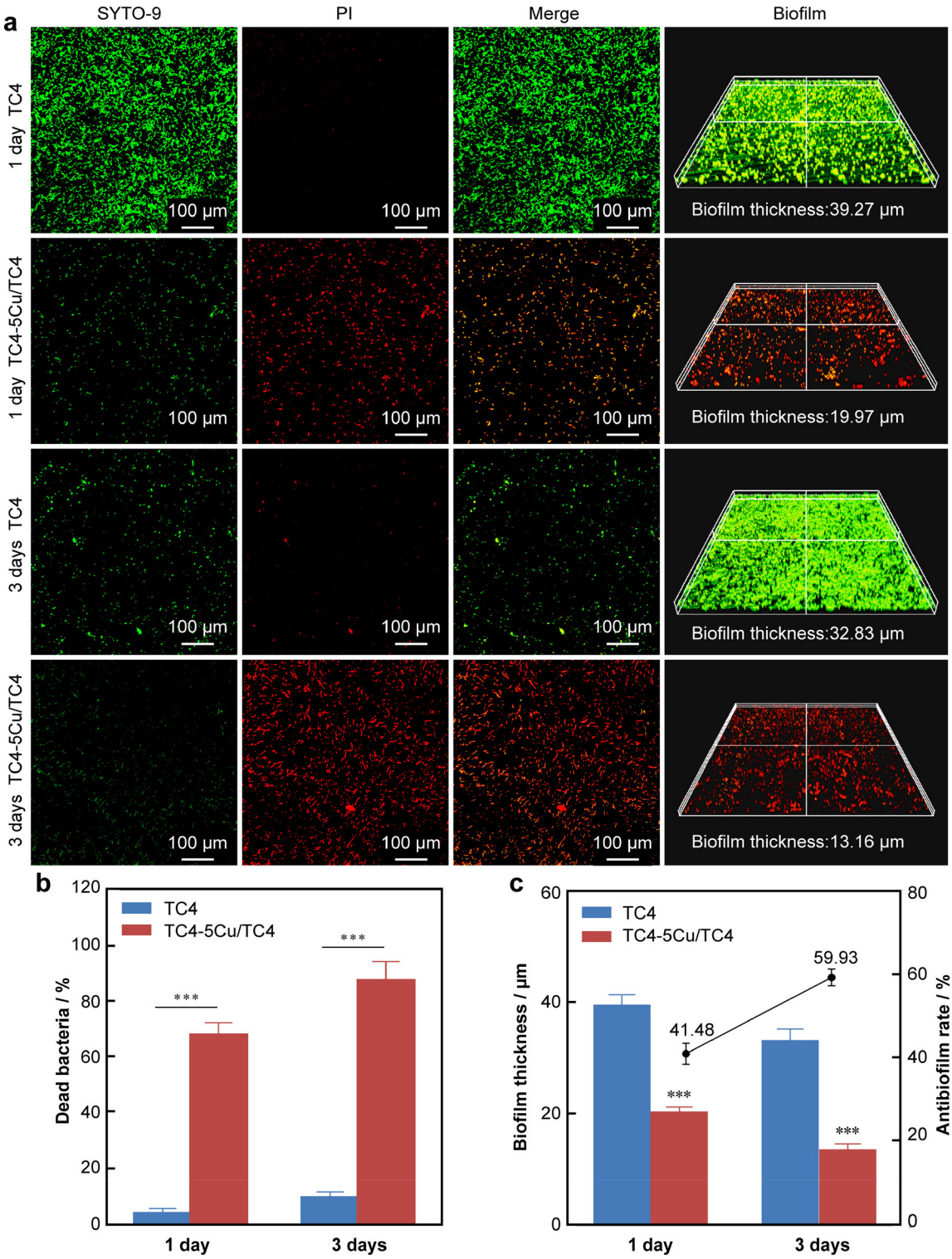

Fig. 9 Sessile bacteria and biofilm observation by CLSM: **a** live and dead staining images of sessile *S. mutans* and bacterial biofilm observation of TC4 and TC4-5Cu/TC4 alloys; **b** quantitative calculation of dead bacteria proportion on samples; **c** biofilm thickness on alloys and antibiofilm rate of TC4-5Cu/TC4 alloy (***$p < 0.001$)

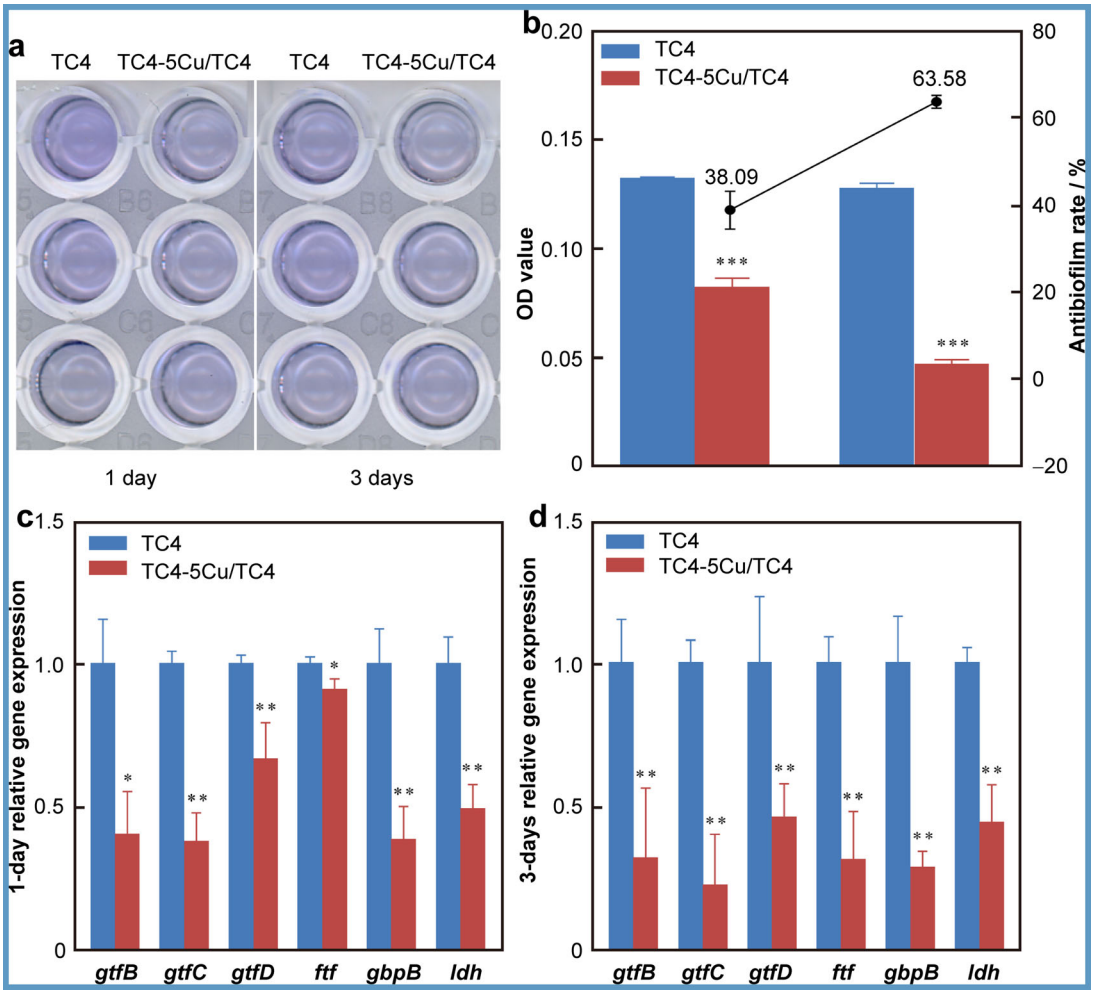

Fig. 10 **a** Anhydrous ethanol dissolved with crystal violet bound to biofilm; **b** crystal violet staining results of *S. mutans* biofilm on different samples and antibiofilm rates of TC4-5Cu/TC4 alloy; relative genes expression of *S. mutans* biofilm on TC4 and TC4-5Cu/TC4 alloys at **c** the first day and **d** the third day (*$p < 0.05$, **$p < 0.01$, ***$p < 0.001$)

4 Discussion

Caries is the most common oral chronic infectious disease mediated by dental plaque biofilm [2]. The biofilm is initially formed by the adhesion and aggregation of bacteria, which erode the tooth tissue [42]. In general, tooth tissues with a treatment device are more likely to adhere to bacteria and then form dental plaque biofilms. In recent years, the development of antibacterial alloys has received more and more attention in order to solve the problem of dental bacterial infection. The copper element has become an attractive component in antibacterial alloys production, due to its strong antibacterial properties and the role of essential trace elements in the human body [23]. However, whether the alloy added with copper element is suitable for fabricating antibacterial dental appliance, it is necessary to study the antibacterial effect of the alloy against *S. mutans*, the most common cariogenic bacteria. In previous studies, titanium alloys with different copper contents (3 wt%, 5 wt% and 7 wt%) were fabricated, and the antibacterial properties and biocompatibility were analyzed. The results demonstrated that the 5 wt% Cu addition presented satisfactory antibacterial effect and biocompatibility [43]. Thus, in this research, 5 wt% copper was added to the TC4 alloy which is widely used in clinic, to product SLMed TC4-5Cu/TC4 alloy, and a series of antibacterial properties against *S. mutans* were analyzed.

The results of material characterization show that the copper element in the TC4-5Cu/TC4 alloy was uniformly distributed within 80 μm of the alloy surface. Meanwhile, the addition of copper had no noticeable effect on the roughness and contact angle of the alloy, which are physical indicator that play an important role in bacterial adhesion [44]. The maximum release concentration of Cu^{2+} in TC4-5Cu/TC4 alloy was 18.73 $\mu g \cdot L^{-1}$ within 30 days, which is far lower than the recommended daily

intake of copper 2–3 mg [45], showcasing that the biosafety of the TC4-5Cu/TC4 alloy is reassuring. However, the MIC and MBC of copper ions were 28.0 and 56.0 $mg{\cdot}L^{-1}$. The value much higher than the release concentration of Cu^{2+} is in line with the result that the alloy did not show antibacterial activity against planktonic bacteria. In addition, it is well known that *S. mutans* produces lactic acid during proliferation and reduces the pH value of the surrounding environment [46]. There was no statistical difference in the pH value of the medium immersed in the two groups of alloys. It was further proved that the TC4-5Cu/TC4 alloy in present work has little antibacterial effect on planktonic bacteria. In contrast, the TC4-5Cu/TC4 alloy exhibits a significant antibacterial effect against sessile bacteria, after incubation for 1 and 3 days. It is speculated that in this research, the Cu^{2+} dissolved in the solution may not be the component that exerts the main antibacterial effect. The contacting sterilization produced by Ti_2Cu phase reported by Liu et al. [39] may be the main antibacterial mechanism of TC4-5Cu/TC4 alloy in this study. The antibacterial experimental data of sessile bacteria also reflected the inhibitory effect of the alloy on the sessile bacteria. The following tests were performed to further understand this effect.

In order to comprehensively evaluate the antibiofilm effect of TC4-5Cu/TC4 alloy against *S. mutans*, SEM observation, CLSM detection and crystal violet measurement were conducted. The observations by SEM and CLSM present that the number of bacteria attached to the TC4-5Cu/TC4 alloy and the proportion of live bacteria were significantly less than those of the TC4 alloy, and the bacterial chain became shorter. It is intuitively reflected the bactericidal effect of the alloy on sessile bacteria and the suppression of the mutual adhesion between *S. mutans*. The measurement of the biofilm thickness by CLSM and the quantitative detection of biofilm by crystal violet clarify that TC4-5Cu/TC4 alloy reduces the formation of biofilm, and the average antibiofilm rates at 1 and 3 days were 38.09% and 63.58%, respectively. It is consistent with the reported results of TC4-5Cu inhibiting the *S. aureus* biofilm formation, verifying the fact that Cu-bearing titanium alloys have broad-spectrum antibacterial and antibiofilm functions [47].

Bacterial biofilm is a three-dimensional structure initial formed by bacteria attached to the material and then coated with EPS [48], and its formation process is regulated by related genes. PCR detection was carried out in order to assess the effects of TC4-5Cu/TC4 alloy on the expression of genes related to *S. mutans* biofilm formation. It was verified that all detected genes were down-regulated, in the TC4-5Cu/TC4 group. Adhesion, aciduricity and acid resistance are the three major virulence factors of *S. mutans* cariogenicity [49]. Bacterial adhesion is the initial stage of biofilm formation and the critical stage of caries development [50]. EPS, especially GTF and FTF, play a significant role in bacterial adhesion and biofilm formation. GTF decomposes sucrose into glucose and fructose and then catalyzes the synthesis of dextran from glucose, while fructose is catalyzed by FTF to fructan [51]. Glucan mainly promotes the formation of biofilm by enhancing the mutual adhesion of bacteria and the attachment of bacteria to the saliva acquired membrane. Studies have shown that the biofilm formation ability and cariogenicity of *S. mutans* lacking the *gtf* gene are significantly reduced [52]. In addition to the ability to assist in the formation of biofilms, fructans are also responsible for storing nutrients for bacteria to prevent death in the sucrose deficiency stage [12]. Except for the above-mentioned genes, the biofilm formation is also affected by GbpB, the product of the *gpbB* gene. Based on reports, *S. mutans* with *gbpB* gene defect grows slowly down and is less likely to form long chains [15, 53]. Combining with the above evaluation of antibiofilm, it is speculated that the reduction of sessile bacteria and biofilm thickness are inseparably related to the down-regulation of corresponding gene expression. In addition to genes that regulate biofilm formation, the expression of the acid production gene *ldh* was also tested. Lactic acid produced by *S. mutans* is a key component of its destruction of tooth tissue [16, 54]. The down-regulation of *ldh* gene indicates that TC4-5Cu/TC4 alloy can not only inhibit the formation of biofilm of *S. mutans*, but also reduce the ability of acid production and the damage to teeth.

5 Conclusion

In this work, a gradient TC4-5Cu/TC4 alloy was successfully manufactured using SLM technology. Experimental results showed that the Cu addition had little effect on the roughness and contact angle of the alloy. The TC4-5Cu/TC4 alloy exhibited significant antibiofilm property against *S. mutans*. Namely, the alloy showed outstanding antibacterial efficacy against sessile bacteria, but almost no antibacterial activity against planktonic bacteria. This observation can be explained by the fact that the Cu^{2+} leakage was much lower than the MIC and MBC of Cu^{2+}. The result of RT-PCR demonstrates that TC4-5Cu/TC4 alloy reduced the pathogenicity of *S. mutans* by down-regulating the expression of genes related to bacterial adhesion and acid production. Based on the above results and discussion, TC4-5Cu/TC4 alloy has brighter prospects in the development of dental device materials for preventing dental caries.

Acknowledgements This study was financially supported by the National Natural Science Foundation of China (No. 51871050), the Natural Science Foundation Project of Liaoning Province (Nos. 2020-MS-150 and 2018225059) and Shenyang Science and Technology Funded Project (No. RC190290).

Declarations

Conflict of interests The authors declare that they have no conflict of interests.

References

[1] Sharma A, Agarwal N, Anand A, Jabin Z. To compare the effectiveness of different mouthrinses on *Streptococcus mutans* count in caries active children. J Oral Biol Craniofac Res. 2018; 8(2):113.
[2] Selwitz RH, Ismail AI, Pitts NB. Dental caries. Lancet. 2007; 369(9555):51.
[3] Liu BH, Yu LC. In-situ, time-lapse study of extracellular polymeric substance discharge in *Streptococcus mutans* biofilm. Colloids Surf B Biointerfaces. 2017;150:98.
[4] Kuang XY, Chen VV, Xu X. Novel approaches to the control of oral microbial biofilms. Biomed Res Int. 2018;2018:6498932.
[5] Ong KS, Mawang CI, Daniel-Jambun D, Lim YY, Lee SM. Current anti-biofilm strategies and potential of antioxidants in biofilm control. Expert Rev Anti Infect Ther. 2018;16(11):855.
[6] Krzyściak W, Jurczak A, Kościelniak D, Bystrowska B, Skalniak A. The virulence of *Streptococcus mutans* and the ability to form biofilms. Eur J Clin Microbiol Infect Dis. 2014;33(4):499.
[7] Durso SC, Vieira LM, Cruz JN, Azevedo CS, Rodrigues PH, Simionato MR. Sucrose substitutes affect the cariogenic potential of *Streptococcus mutans* biofilms. Caries Res. 2014;48(3): 214.
[8] Bowen WH. Dental caries: not just holes in teeth! A perspective. Mol Oral Microbiol. 2016;31(3):228.
[9] Gabe V, Kacergius T, Abu-Lafi S, Kalesinskas P, Masalha M, Falah M, Abu-Farich B, Melninkaitis A, Zeidan M, Rayan A. Inhibitory effects of ethyl gallate on *Streptococcus mutans* biofilm formation by optical profilometry and gene expression analysis. Molecules. 2019;24(3):529.
[10] De A, Jorgensen AN, Beatty WL, Lemos J, Wen ZT. Deficiency of MecA in *Streptococcus mutans* causes major defects in cell envelope biogenesis, cell division, and biofilm formation. Front Microbiol. 2018;9:2130.
[11] Veloz JJ, Saavedra N, Alvear M, Zambrano T, Barrientos L, Salazar LA. Polyphenol-rich extract from propolis reduces the expression and activity of *Streptococcus mutans* glucosyltransferases at subinhibitory concentrations. Biomed Res Int. 2016; 2016:4302706.
[12] Li YH, Burne RA. Regulation of the *gtfBC* and *ftf* genes of *Streptococcus mutans* in biofilms in response to pH and carbohydrate. Microbiology (Reading). 2001;147(Pt 10):2841.
[13] Guan CR, Che FA, Zhou HX, Li YW, Li YR, Chu JP. Effect of rubusoside, a natural sucrose substitute, on *Streptococcus mutans* biofilm cariogenic potential and virulence gene expression in vitro. Appl Environ Microbiol. 2020;86(16):e01012.
[14] Duque C, Stipp RN, Wang B, Smith DJ, Höfling JF, Kuramitsu HK, Duncan MJ, Mattos-Graner RO. Downregulation of GbpB, a component of the VicRK regulon, affects biofilm formation and cell surface characteristics of *Streptococcus mutans*. Infect Immun. 2011;79(2):786.
[15] Fujita K, Takashima Y, Inagaki S, Nagayama K, Nomura R, Ardin AC, Grönroos L, Alaluusua S, Ooshima T, Matsumoto-Nakano M. Correlation of biological properties with glucan-binding protein B expression profile in *Streptococcus mutans* clinical isolates. Arch Oral Biol. 2011;56(3):258.
[16] He ZY, Huang ZW, Jiang W, Zhou W. Antimicrobial activity of cinnamaldehyde on *Streptococcus mutans* biofilms. Front Microbiol. 2019;10:2241.
[17] Ahn SJ, Lim BS, Lee SJ. Prevalence of cariogenic streptococci on incisor brackets detected by polymerase chain reaction. Am J Orthod Dentofacial Orthop. 2007;131(6):736.
[18] Arunachalam LT, Merugu S, Sudhakar U. Comparison of intraoral distribution of two commercially available chlorhexidine mouthrinses with and without alcohol at three different rinsing periods. J Int Soc Prev Community Dent. 2012;2(1): 20.
[19] Takenaka S, Ohsumi T, Noiri Y. Evidence-based strategy for dental biofilms: current evidence of mouthwashes on dental biofilm and gingivitis. Jpn Dent Sci Rev. 2019;55(1):33.
[20] Zhang JM, Sun YH, Zhao Y, Liu YL, Yao XH, Tang B, Hang RQ. Antibacterial ability and cytocompatibility of Cu-incorporated Ni–Ti–O nanopores on NiTi alloy. Rare Met. 2019;38(6): 552.
[21] Xiang YM, Li J, Liu XM, Cui ZD, Yang XJ, Yeung KWK, Pan HB, Wu SL. Construction of poly (lactic-co-glycolic acid)/ZnO nanorods/Ag nanoparticles hybrid coating on Ti implants for enhanced antibacterial activity and biocompatibility. Mater Sci Eng C Mater Biol Appl. 2017;79:629.
[22] Lu YJ, Ren L, Xu XC, Yang Y, Wu SQ, Luo JS, Yang MY, Liu LL, Zhuang DH, Yang K, Lin JX. Effect of Cu on microstructure, mechanical properties, corrosion resistance and cytotoxicity of CoCrW alloy fabricated by selective laser melting. J Mech Behav Biomed Mater. 2018;81:130.
[23] Zhang EL, Fu S, Wang RX, Li HX, Liu Y, Ma ZQ, Liu GK, Zhu XS, Qin GW, Chen DF. Role of Cu element in biomedical metal alloy design. Rare Met. 2019;38(6):476.
[24] Zhang D, Han Q, Yu K, Lu XP, Liu Y, Lu Z, Wang Q. Antibacterial activities against *Porphyromonas gingivalis* and biological characteristics of copper-bearing PEO coatings on magnesium. J Mater Sci Technol. 2021;61(2):33.
[25] Vincent M, Duval RE, Hartemann P, Engels-Deutsch M. Contact killing and antimicrobial properties of copper. J Appl Microbiol. 2018;124(5):1032.
[26] Zhang EL, Wang XY, Chen M, Hou B. Effect of the existing form of Cu element on the mechanical properties, bio-corrosion and antibacterial properties of Ti-Cu alloys for biomedical application. Mater Sci Eng C Mater Biol Appl. 2016;69:1210.
[27] Li HF, Qiu KJ, Zhou FY, Li L, Zheng YF. Design and development of novel antibacterial Ti-Ni-Cu shape memory alloys for biomedical application. Sci Rep. 2016;6:37475.
[28] Chen LM, Yu HY, Deutschman C, Yang T, Tam KC. Novel design of Fe-Cu alloy coated cellulose nanocrystals with strong antibacterial ability and efficient Pb^{2+} removal. Carbohydr Polym. 2020;234:115889.
[29] Wu JH, Chen KK, Chao CY, Chang YH, Du JK. Effect of Ti_2Cu precipitation on antibacterial property of Ti-5Cu alloy. Mater Sci Eng C Mater Biol Appl. 2020;108:110433.
[30] Alshammari Y, Yang F, Bolzoni L. Low-cost powder metallurgy Ti-Cu alloys as a potential antibacterial material. J Mech Behav Biomed Mater. 2019;95:232.
[31] Egorkin VS, Medvedev IM, Sinebryukhov SL, Vyaliy IE, Gnedenkov AS, Nadaraia KV, Izotov NV, Mashtalyar DV, Gnedenkov SV. Atmospheric and marine corrosion of PEO and composite coatings obtained on Al-Cu-Mg aluminum alloy. Materials (Basel). 2020;13(12):2739.
[32] Unabia RB, Candidato RT Jr, Pawłowski L, Salvatori R, Bellucci D, Cannillo V. In vitro studies of solution precursor plasma-sprayed copper-doped hydroxyapatite coatings with

increasing copper content. J Biomed Mater Res B Appl Biomater. 2020;108(6):2579.
[33] Babu P, Naik B. Cu-Ag bimetal alloy decorated SiO_2@ TiO_2 hybrid photocatalyst for enhanced H_2 evolution and phenol oxidation under visible light. Inorg Chem. 2020;59(15):10824.
[34] Taira M, Moser JB, Greener EH. Studies of Ti alloys for dental casting. Dent Mater. 1989;5(1):45.
[35] Abranches J, Zeng L, Kajfasz JK, Palmer SR, Chakraborty B, Wen ZT, Richards VP, Brady LJ, Lemos JA. Biology of oral *Streptococci*. Microbiol Spectr. 2018;6(5):GPP3-0042–2018.
[36] Tamura S, Yonezawa H, Motegi M, Nakao R, Yoneda S, Watanabe H, Yamazaki T, Senpuku H. Inhibiting effects of *Streptococcus salivarius* on competence-stimulating peptide-dependent biofilm formation by *Streptococcus mutans*. Oral Microbiol Immunol. 2009;24(2):152.
[37] Zong WA, Zhang S, Zhang CH, Ren L, Wang Q. Design and characterization of selective laser-melted Ti6Al4v-5Cu alloy for dental implants. Mater Corros. 2020. https://doi.org/10.1002/maco.202011650.
[38] Meng YY, Zhang D, Jia XY, Xiao KS, Lin X, Yang Y, Xu DK, Wang Q. Antimicrobial activity of nano-magnesium hydroxide against oral bacteria and application in root canal sealer. Med Sci Mon. 2020. https://doi.org/10.1265/MSM.922920.
[39] Liu R, Tang YL, Zeng LL, Zhao Y, Ma Z, Sun ZQ, Xiang LB, Ren L, Yang K. In vitro and in vivo studies of anti-bacterial copper-bearing titanium alloy for dental application. Dent Mater. 2018;34(8):1112.
[40] Zhou EZ, Qiao DX, Yang Y, Xu DK, Lu YP, Wang JJ, Smith JA, Li HB, Zhao HL, Liaw PK, Wang FH. A novel Cu-bearing high-entropy alloy with significant antibacterial behavior against corrosive marine biofilms. J Mater Sci Technol. 2020;46:201.
[41] Zhuang YF, Ren L, Zhang SY, Wei X, Yang K, Dai KR. Antibacterial effect of a copper-containing titanium alloy against implant-associated infection induced by *methicillin-resistant Staphylococcus aureus*. Acta Biomater. 2021;119:472.
[42] Bowen WH, Koo H. Biology of *Streptococcus mutans*-derived glucosyltransferases: role in extracellular matrix formation of cariogenic biofilms. Caries Res. 2011;45(1):69.
[43] Zhang W, Zhang SY, Liu H, Ren L, Wang Q, Zhang Y. Effects of surface roughening on antibacterial and osteogenic properties of Ti-Cu alloys with different Cu contents. J Mater Sci Technol. 2021;88:158.
[44] Bilgili D, Dündar A, Barutçugil Ç, Tayfun D, Özyurt ÖK. Surface properties and bacterial adhesion of bulk-fill composite resins. J Dent. 2020;95:103317.
[45] Harris ED. Basic and clinical aspects of copper. Crit Rev Clin Lab Sci. 2003;40(5):547.
[46] Richards VP, Alvarez AJ, Luce AR, Bedenbaugh M, Mitchell ML, Burne RA, Nascimento MM. Microbiomes of site-specific dental plaques from children with different caries status. Infect Immun. 2017;85(8):e00106.
[47] Li M, Ma Z, Zhu Y, Xia H, Yao MY, Chu X, Wang XL, Yang K, Yang MM, Zhang Y, Mao CB. Toward a molecular understanding of the antibacterial mechanism of copper-bearing titanium alloys against *Staphylococcus aureus*. Adv Healthc Mater. 2016;5(5):557.
[48] Florez Salamanca EJ, Klein MI. Extracellular matrix influence in *Streptococcus mutans* gene expression in a cariogenic biofilm. Mol Oral Microbiol. 2018;33(2):181.
[49] Cui T, Luo WF, Xu LT, Yang BQ, Zhao W, Cang HX. Progress of antimicrobial discovery against the major cariogenic pathogen *Streptococcus mutans*. Curr Issues Mol Biol. 2019;32:601.
[50] Kreth J, Merritt J, Qi F. Bacterial and host interactions of oral streptococci. DNA Cell Biol. 2009;28(8):397.
[51] Monchois V, Willemot RM, Monsan P. Glucansucrases: mechanism of action and structure-function relationships. FEMS Microbiol Rev. 1999;23(2):131.
[52] Koo H, Xiao J, Klein MI, Jeon JG. Exopolysaccharides produced by *Streptococcus mutans* glucosyltransferases modulate the establishment of microcolonies within multispecies biofilms. J Bacteriol. 2010;192(12):3024.
[53] Fujita K, Matsumoto-Nakano M, Inagaki S, Ooshima T. Biological functions of glucan-binding protein B of *Streptococcus mutans*. Oral Microbiol Immunol. 2007;22(5):289.
[54] Bijle MN, Neelakantan P, Ekambaram M, Lo ECM, Yiu CKY. Effect of a novel synbiotic on *Streptococcus mutans*. Sci Rep. 2020;10(1):7951.